Journal of Engineering Science and Technology
Special Issue on SOMCHE 2014 & RSCE 2014 Conference, January (2015) 17 - 23

PRODUCTION OF SUPERHYDROPHOBIC GALVANIZED IRON PLATE VIA ELECTRODEPOSITION METHOD

J. F. T. BADIOLA, G. A. GUERRERO, J. R. AMORES,
J. D. M. PLANAS, R. PACHECO, E. C. ROQUE*

Adamson University, 900 San Marcelino Street Ermita, 1000 Manila, Philippines
*Corresponding Author: erison.roque@adamson.edu.ph

Abstract

This study aimed to developed a superhydrophobic substance and apply it to the surface of a galvanized iron. Using electrodeposition, the researchers have produced a superhydrophobic surface in a cathodic surface by electrodepositing it in a galvanized iron plate. The electrodeposition process utilizes an electrolytic solution of manganese chloride ($MnCl_2 4H_2O$), myristic acid ($CH_3(CH_2)_{12}COOH$) and 95% ethanol for 15 minutes in 30V. Using SEM (Scanning Electron Microscope) to characterize the superhydrophobic surface, the researchers found out that it was made of cluster of microscale particles which were composed of many smaller nanoparticles which allows the superhydrophobic surface to store a lot of air thus prevents water from entering or contacting the surface. Using FTIR (Fourier Transform Infrared Spectroscopy), the researchers determined that the superhydrophobic surface in the cathodic surface is composed of Mn myristate ($Mn[CH_3 (CH_2)_{12} COO]_2$). The superhydrophobic surface was attributed to its contact angle measuring at 150º or greater which made the water in contact with it to occupy a minimum area of contact thus this can be easily removed at a tilting or rolling angle of less than 3º.

Keywords: Superhydrophobic, Electrodepositing, Electrolyte.

1. Introduction

One of the factors affecting the superhydrophobicity of a surface is wettability, which is one of the fundamental properties of solid surfaces and controlling the wettability of a surface is an important problem relevant to daily life, agriculture, industry and fundamental research. When it comes to wettability of a surface, one interesting topic is the superhydrophobic surface due to its promising applications [1]. It is generally accepted that superhydrophobic and self-cleaning properties are based on the hierarchical roughness of the surface on a micro and nano scale, combined with the chemistry of low surface energy compounds. Water forms spherical droplets on such surfaces with a high contact angle (> 150°), and can easily roll of the surface taking with it dust particles [2]. Fabrications of synthetic superhydrophobic surfaces based on polymers, metals, metal oxides, carbon nanotubes and waxes, which mimic the properties of "lotus" surface, have been reported in recent years. Techniques commonly employed are states that Electrochemical oxidation, chemical etching, chemical and electrochemical deposition, plasma etching, plasma deposition, laser ablation, chemical vapour deposition (CVD) and sol–gel processing [3]. However, in this research study the electrodepostion method will be used due to its cheapness and fast one-step process.

The superhydrophobic and self-cleaning properties induced by surface roughness are widely adopted in nature, including plant leaves, butterfly wings, and water strider legs. There are hundreds of different plants with the ability to completely clean their leaves from contamination (dust particle, spores and pathogens) by a simple rain shower or fog [4]. Among these plants, the most impressive example is the Lotus plant (Nelumbo nucifera) in which the superhydrophobic properties were first documented and named as the "lotus effect" [5]. A combination of hydrophobicity and micro- or nano scale surface roughness can result in an effect known as superhydrophobicity, which was characterized by water droplets beading on the solid surface at contact angles exceeding 150°. It was also pointed out that when fully submersed in water, such surface can cause so called "slip effect," resulting in significant reduction in the skin-friction drag exerted on the surface [6]. Thus finding a noble way to produce a superhydrophobic surface is a must and application of such can lead to many engineering applications. Superhydrophobic coatings can be utilized as a passive method of flow control and may potentially become a viable alternative to the more complex and energy consuming active or reactive flow control techniques such as wall suction/blowing.

2. Experimental

For this study, analytical reagents of 95% ethanol, manganese chloride and myristic acid were used and obtained from Patagonian Enterprises. Galvanized iron plates of 5 cm x 2 cm x 1 mm were used as electrodes in the electrodeposition process using a 30 V from a DC power source. Galvanized iron plates were also obtained from Patagonian Enterprises. A silicon carbide with medium-grit will be used to abrade the galvanized iron and an etching solution of 20% wt. HCl will be used using the HCl solution in Adamson University Chemical Engineering Laboratory. Also, Fourier-Transform Infrared Spectroscopy of Adamson University and Scanning Electron Spectroscopy of De LaSalle University will be used for composition and surface analysis.

2.1. Chemical functional group

FTIR spectra were employed to analyze the chemical composition of the as-prepared cathodic superhydrophobic surfaces (SHS). Table 1 reveals the chemical groups for three (3) samples of the superhydrophobic surface with FTIR spectra. In the high frequency region, the spectrum of superhydrophobic surface exhibits the average adsorption peaks at about 2917.87 cm^{-1}, which is, attributed to C–H asymmetric and symmetric stretching vibrations. In the low frequency region, it is well known that the carboxyl group (COO) from myristic acid appears at 1701 cm^{-1}. While the superhydrophobic surfaces exhibit the adsorption peaks at an average of 1561.06 cm^{-1}. The two adsorption peaks may stem from asymmetric and symmetric stretches of –COO group. Thus based on the FTIR analysis, we can deduce that Mn myristate ($Mn[CH_3 (CH_2)_{12} COO]_2$) with low surface energy is formed on the superhydrophobic surfaces. According to Zhu et al. [7] the surface wettability is controlled by the chemical components, as well as surface roughness, of the solids.

Table 1. High Frequency Region and Low Frequency Region of the Superhydrophobic Surfaces of Sample 1, 2 and 3.

	High Frequency Region Wave number (cm^{-1})	Low Frequency Region Wave number (cm^{-1})
Sample 1	2917.7	1562.35
Sample 2	2917.69	1562.25
Sample 3	2917.47	1558.59

2.2. Surface morphology

As shown in Figs. 1-3 the surfaces of the superhydrophobic galvanized iron plate are composed of micro/nano structures. It can be further seen from high magnification SEM images (50 micrometer and 10 micrometer) that the micro/nano structures are composed of even smaller nano structures in the three (3) samples. As shown in the images below, the cluster of structures represents the surface of the sample's sharp edges and hierarchical structures of the three (3) samples that consist of minute particles, which have clusters of microscale particles that allow the surface to have spaces in between the sharp edges. According to Feng et al. [8] the spaces produced by superhydrophobic surface allows air to fill up the said free volume thus preventing the water to fill in. According to the Zhuo et al. [9] these hierarchical structures is a crucial factor for the effectiveness of the superhydrophobic surface. In another journal by Feng et al. [8] these rough hierarchical structures can trap large fraction of air within the micro and nano textured surfaces. The trapped air can greatly increase the air/liquid interface, which prevents the penetration of water droplets into the groves of the surface resulting in high water contact and tilting angle.

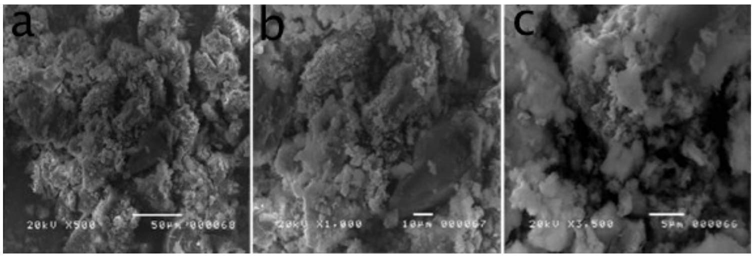

Fig. 1. Sample 1 Superhydrophobic Galvanized Iron Plate SEM Images in (a) 50µm; (b) 10µm; (c) 5µm.

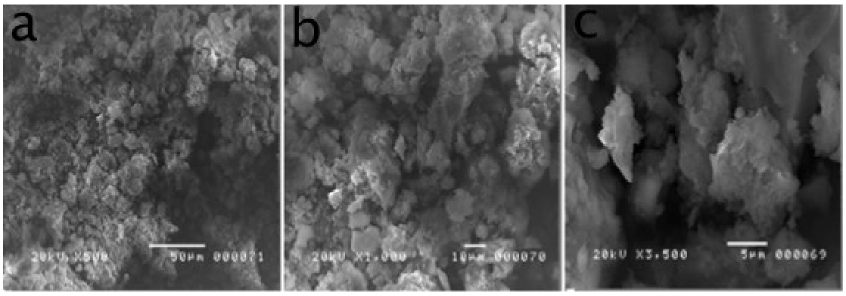

Fig. 2. Sample 2 Superhydrophobic Galvanized Iron Plate Sem Images in (a) 50μm; (b) 10μm; (c) 5μm.

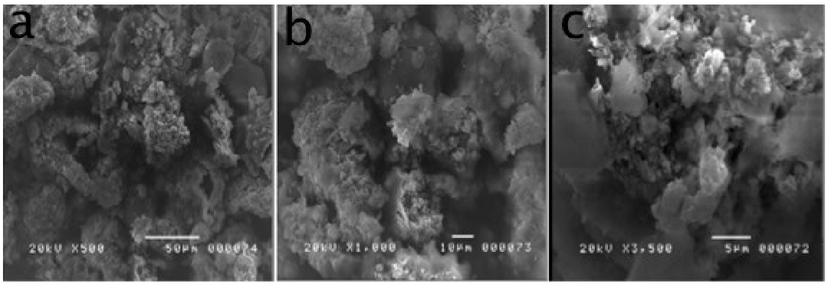

Fig. 3. Sample 3 Superhydrophobic Galvanized Iron Plate Sem Images in (a) 50μm; (b) 10μm; (c) 5μm.

2.3. Contact angle and tilting angle measuring

By using a Vernier caliper, the height and diameter of the water droplet sitting on the superhydrophobic surface could be measured. Using the drop shape method calculation its contact angle could be measured. The tilting angle is obtained by measuring the elevation of the plate make with the horizontal plane. The contact and tilting angle of uncoated and superhydrophobic galvanized iron plate sample 1, sample 2 and sample 3 is tabulated in Table 2.

Table 2. Contact and Tilting Angle of Uncoated, Sample 1 SHS, Sample 2 SHS and Sample 3 SHH.

Sample	Diameter (cm)	Height (cm)	Contact Angle	Tilting Angle	
				Height (cm)	Angle
Uncoated	0.612	0.553	120.3	X	X
1	0.303	0.577	150.6	0.262	3
2	0.336	0.694	152.8	0.253	2.9
3	0.325	0.642	151.6	0.244	2.8

As shown in the results superhydrophobic galvanized iron plate has a significant increase of 26.1% having an average of 151.67^o and 2.9^o in its contact and tilting angle, respectively. This increase in its contact and tilting angle is the effect of the hierarchical structures in its surface which contains smaller nano structures. According to Feng [8] superhydrophibic surfaces exhibit more hydrophobicity if hierarchical structure is present due to the allowance of air volume. Due to the hierarchical structures of the superhydrophobic surface, the water droplet on top of the superhydrophobic surface occupied a minimum amount of surface area creating a high contact angle of greater than 150° and allowing it to be easily removed at a sliding angle of less than 3°. This is supported by a similar study of Feng [8], "the micro and nanostructures not only enhance the surface hydrophobicity but also reduce CA hysteresis, which is crucial to the self cleaning properties of these surfaces. This observation can be attributed to the following reasons: first, the hierarchical structure decreases the contact area between solid and water at their interface and causes a higher water CA and low tilting angle."

3. Conclusions

A production of superhydrophobic cathodic surface has been made by electrodepositing galvanized iron plate in an electrolyte solution containing manganese chloride ($MnCl_2 \cdot 4H_2O$), myristic acid ($CH_3(CH_2)_{12}COOH$) and ethanol. This is characterized using fourier-transform infrared spectroscopy and scanning electron microscopy. Some concluding observations from the investigation are given below:

- The superhydrophobic surfaces are composed of minute particles. Within these minute particles are cluster of microscale particles which allow the superhydrophobic surface to have spaces in between the sharp edges at the surface.
- The superhydrophobic surfaces that are produced have an average wave numbers of 1561.06 cm^{-1} and 2917.62 cm^{-1} in the low and high frequency region, respectively. Thus the particles in the surface are made up of Mn myristate ($Mn[CH_3 (CH_2)_{12} COO]_2$) with low surface energy.
- The fabricated surfaces that have been produced have an average contact angle of 151.67^o that is considerably high thus the surface is superhydrophibic.
- The superhydrophobic surfaces that have been fabricated have an average tilting angle of 2.9^o. For a superhydrophobic surface to be effective it should have a required tilting angle of 3^o or less to make the water droplet sitting on it to slide across its surface. Thus the suface has high superhydrophobicity effectiveness.
- The distance between sharp surfaces of the superhydrophobic surfaces has formed in the structure of the surface, which contributed to its superhydrophobic property.

Acknowledgement

This work was sponsored by the Center for Research and Continuing Education (CRECE) of Adamson University.

References

1. Baxter, D.K.; Chen, X.G.; and Huang, Y. (2011). Fabrication of superhydrophobic surfaces on aluminum alloy via electrodeposition of copper followed by electrochemical modification. *Nano-Micro Letter*, 3(3), 160-165.
2. Bai, H.; Fung, G.; and Li, C. (2008). Electrochemical fabrication of superhydrophobic surfaces on metal and semiconductor substrates. *Journal of Adhesion Science and Technology*, 22(15), 1819-1839.
3. Han, T.Y.; Huang, W.J.; and Lee, T.C. (2009). Preparation of a superhydrophobic ZnO film on ITO Glass via electrodeposition followed by oxidation. effect of the deposition time. *Journal of Adhesion Science and Technology* 23(13-14), 1799-1810.
4. Bushan, Z.; Li, T.; Liu, C.; and Zhang, Q. (2009). Sticky and slippy: two hydrophobic states transition of ZnO hierarchical films by Flouroalkylsilane modification. *International Journal of Modern Physics B - IJMPB*, 23(6-7), 1867-1872.
5. Barthlott J.; Chang, Y.Y.; Hung, Y.L.; Lin, S.Y.; and Wang, M.J. (2010). A simple method for measuring the superhydrophobic contact angle with high accuracy. *Review of Scientific Instruments*, 81(6), 1-8.
6. Chang, F.M.; Ruthstein, H.K.; and Sheng, Y.J. (2009). Superhydrophobic floatability of a hydrophilic object driven by edge effect. *Applied Physics Letter*, 95, 17-24.
7. Feng, Y.; Ye, X.; Zhou, Z.; and Zhu, L. (2005). Tuning wettability and getting superhydrophobic surface by controlling surface roughness with well-designed microstructures. *Sensors and Actuators A-physical*, 130, 595-600.
8. Feng, L.; Jiang, L.; and Xi, J. (2008). A general approach for fabrication of superhydrophobic and superamphiphobic surfaces. *Applied Physics Letter* 92, 13-16.
9. Brown, J.; Lin, Z.W.; and Zhou, Y.P. (2009). Superhydrophobic surfaces for water-repellent or self-cleaning. *Surface Review and Letters*, 16(16), 645-652.

Appendix A

Angle Measurement

A.1. Contact Angle Measurement

Measure height and diameter of the droplet. For the standard illustrated, the height was 0.577 cm and diameter was 0.303 cm. The contact angle, q, is given by geometry:

$q = 2\tan^{-1}(2\text{height}/d)$

$q = 2\tan^{-1}[(2*0.577)/0.303]=150.6^o$

A.2. Tilting angle measurement

$\theta = \text{arcsine}(h/5)$

$\theta = \text{arcsine}(0.262/5) = 3°$

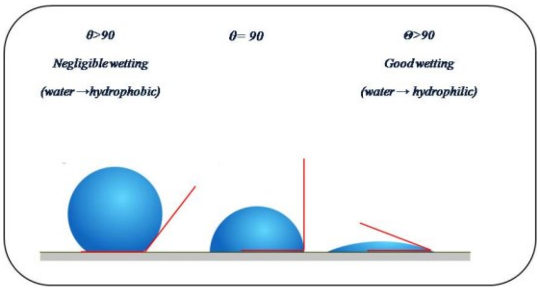

Fig. A-1. Illustration of Hydrophobicity in terms of Contact Angle.

Appendix B

Fourier Transform Infrared Spectroscopy Results

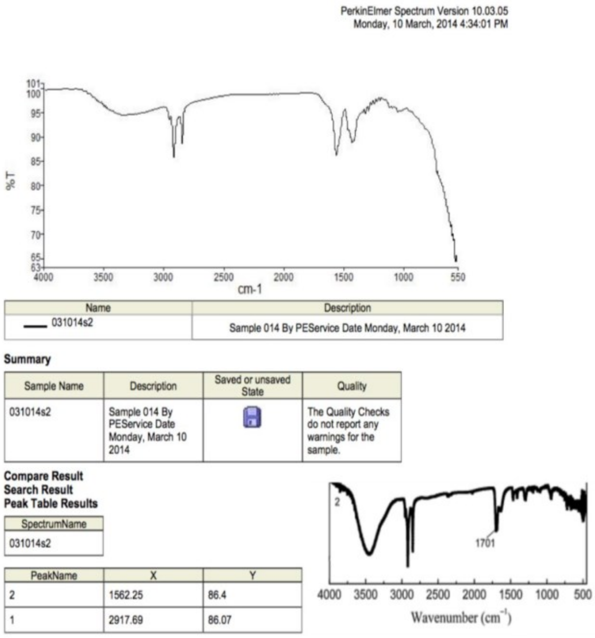

Name	Description
031014s2	Sample 014 By PEService Date Monday, March 10 2014

Summary

Sample Name	Description	Saved or unsaved State	Quality
031014s2	Sample 014 By PEService Date Monday, March 10 2014		The Quality Checks do not report any warnings for the sample.

Compare Result
Search Result
Peak Table Results

SpectrumName
031014s2

PeakName	X	Y
2	1562.25	86.4
1	2917.69	86.07

Fig. B-1. Results of Fourier Transform Infrared Spectroscopy.